Rheology of Reactively Compatibilized Polymer Blends with Varying Extent of Interfacial Reaction

Himanshu Asthana and K. Jayaraman*

Department of Chemical Engineering, Michigan State University, East Lansing, Michigan 48824

Received February 6, 1998; Revised Manuscript Received February 18, 1999

ABSTRACT: This paper presents the rheology and morphology of immiscible polymer blends compatibilized by a polymer reaction at the interface. Nylon-6 was melt blended in a twin screw extruder with several different grades of maleated polypropylene at 10 and 20 wt %. The extent of polymer reaction at the interface is varied by varying the extent of maleation of polypropylene and affects the phase morphology differently at different phase volume fractions. The rheology of the reactive blends is fit to the Palierne theory to infer values of the equilibrium interfacial tension. The equilibrium interfacial tension of the reactive blends is reduced in proportion to the extent of maleation of the polypropylene. In blends with more reaction product, another mechanical property of the interface is required to fit the low-frequency data well.

1. Introduction

Blending of polymers is a popular method of improving their end-use properties.[1] However, most polymers are thermodynamically incompatible and phase separate on blending. Compatibilization of polymer blends is carried out to reduce the scale of dispersion and to stabilize the morphology. This can be achieved by addition of a premade block copolymer to the system or by carrying out an in-situ reaction between the complementary groups of the blend components. Both techniques promote dispersive mixing which leads to a reduced particle size.

Experimental evidence suggests that the addition of premade block copolymers leads to a reduction of interfacial tension.[2−4] But in the area of reactive blending, experimental results showing the quantitative effects of interfacial reaction on interfacial tension are limited. In a study on blending of nylon-6 with nonreactive and reactive rubbers, Wu[5] predicted that the interfacial tension could drop from 8 mN/m in a nonreactive blend to 0.25 mN/m in reactive blends. The prediction was based on a statistical mechanical theory of polymer interfaces due to Helfand and Tagami.[6] This theory predicts the relation shown in eq 1.

$$\Gamma^\circ \propto 1/L \tag{1}$$

where Γ° is the equilibrium interfacial tension and L is the interfacial thickness. The Helfand theory was developed for a "bare interface", i.e., an interface that has not been occupied by a copolymer or a reacted moiety. Wu arrived at the following modified result on the basis of interfacial thickness and interfacial tension in model experimental systems. This empirical rule

$$\Gamma^\circ \propto 1/L^{0.86} \tag{2}$$

was then combined with measurements of interfacial thickness in nylon-6−reactive rubber blends to obtain a value of 0.25 mN/m for interfacial tension in these systems. One of the aims of this study is to obtain values of interfacial tension independent of interfacial thickness measurements, in reactively blended polymer systems.

An important effect of the interfacial reaction is the modification of the interface from a "bare interface" to an "occupied interface". As the extent of interfacial reaction increases, the interface is progressively occupied. Fayt and co-workers[7] have reported that the addition of a block copolymer leads to a broader interface. The interface may have many layers of molecules. In a recent theoretical paper, O'Shaughnessy and Sawhney[8] conclude that, besides reducing interfacial tension, an "occupied interface" also suppresses coalescence. This is a direct result of steric hindrance provided by the "occupied interface" and leads to a stabilization of the morphology. The experimental evidence presented by Sundararaj and Macosko[9] corroborates this conclusion. In this study we will investigate the effect of increased occupation of the interface by successively increasing the extent of polymer reaction. Thus, to sum up, there are two important issues being investigated in this work: (i) What is the effect of interfacial reaction on the interfacial tension in polymer blends? (ii) What is the effect of "progressive crowding" at the interface on the rheological behavior of the blend?

In this study, nylon-6 has been blended with polypropylene maleated to different extents. Increasing extent of maleation leads to increasing extent of interfacial reaction and hence "progressive crowding" at the interface.

2. Models of Emulsion Rheology

The classic theory of rheology of emulsions focuses on dilute emulsions of spherical, Newtonian drops; see e.g. Frankel and Acrivos[10] and Schowalter et al.[11] The parameters in this theory are the capillary number Ca and the viscosity ratio k, defined as follows in terms of

* To whom correspondence must be addressed.

10.1021/ma980181d CCC: $18.00
Published on Web 04/24/1999

the drop radius R, the strain rate $\dot{\gamma}$, the equilibrium interfacial tension, and the viscosities of the two phases.

$$\mathrm{Ca} = \frac{\eta_m \dot{\gamma} R}{\Gamma^\circ} = \frac{\text{viscous forces}}{\text{interfacial forces}} \tag{3}$$

$$k = \frac{\eta_d}{\eta_m} = \frac{\text{viscosity of the dispersed phase}}{\text{viscosity of the matrix}} \tag{4}$$

These two parameters determine the deformation of the drop D, the ratio of the major axis to minor axis of the distorted spherical drop. Frankel and Acrivos[10] point out that the bulk stress in a flowing emulsion can be predicted well only if the shapes of the dispersed phase agree well with the predicted shapes.

A cell theory for more concentrated emulsions has been reported by Palierne[12] that applies to dynamic shear with very small drop deformation from a spherical shape. Other computational results on concentrated emulsion rheology have been presented by Loewenberg and Hinch[13] for shear flows with appreciable departures from a spherical shape for the dispersed phase. The work of Palierne and of Lowenberg and Hinch cover only a moderate concentration range—up to 0.3. The Palierne theory has an added distinction of being formulated for viscoelastic constituents. However, it is incorrect to use the Palierne model for the large deformation response of emulsions. Two other models of emulsion rheology have been applied widely to polymer blends in the dilute and semidilute regimes to explain their rheological behavior. They are due to Oldroyd[14] and Choi and Schowalter,[15] respectively.

The equilibrium interfacial tension leads to long time relaxation processes affecting the dynamic moduli in the low-frequency region. These long time relaxation processes are associated with the mechanical relaxation of the dispersed phase.[16] The important physical parameters governing the relaxation processes are the viscosity ratio k, the particle radius R, the equilibrium interfacial tension Γ°, and the matrix viscosity η_m. The relaxation time λ_D for the drop shape is given by the following relation.

$$\lambda_D \sim f(k)\frac{R\eta_m}{\Gamma^\circ} \tag{5}$$

The model due to Palierne accounts for the viscoelastic nature of the component phases and the particle size distribution in nondilute emulsions. These factors were not accounted for in the models of Oldroyd and of Choi and Schowalter. The relation for the complex shear modulus of the blend is

$$G^* = G^*_m\left[\frac{1 + {}^3/_2\sum_i \frac{\phi_i E_i}{D_i}}{1 - \sum_i \frac{\phi_i E_i}{D_i}}\right] \tag{6}$$

where

$$E_i = 2(G^*_d - G^*_m)(19G^*_d + 16G^*_m) + \frac{48\beta^*_d\Gamma^\circ}{R_i^2} + \frac{32\beta^*_s(\Gamma^\circ + \beta^*_d)}{R_i^2} + \frac{8\Gamma^\circ}{R_i}(5G^*_d + 2G^*_m) + \frac{2\beta^*_d}{R_i}(23G^*_d - 16G^*_m) + \frac{4\beta^*_s}{R_i}(13G^*_d + 8G^*_m) \tag{7}$$

and

$$D_i = (2G^*_d + 3G^*_m)(19G^*_d + 16G^*_m) + \frac{48\beta^*_d\Gamma^\circ}{R_i^2} + \frac{32\beta^*_s(\Gamma^\circ + \beta^*_d)}{R_i^2} + \frac{40\Gamma^\circ}{R_i}(G^*_d + G^*_m) + \frac{2\beta^*_d}{R_i}(23G^*_d + 32G^*_m) + \frac{4\beta^*_s}{R_i}(13G^*_d + 12G^*_m) \tag{8}$$

The subscript "i" refers to the ith particle fraction. This model explicitly accounts for the rheological properties of the component phases, the volume fraction, the morphology, and the interfacial tension. An interesting feature of this model is its treatment of the interfacial tension as a sum of two parts: an equilibrium interfacial tension Γ° and a frequency-dependent complex part $\beta^*(\omega)$. In turn, $\beta^*(\omega)$ consists of two complex moduli: surface dilatation modulus and surface shear modulus. Both these properties are characteristics of the interface. The surface dilatation modulus is associated with area variations while the surface shear modulus is the resistance of the interface to the shear deformation. The surface shear modulus is related to the layer thickness of the interphase. If $\beta^*(\omega)$ equals 0, the model takes the reduced form shown in eq 9.

$$G^*(\omega) = G^*_m(\omega)\frac{1 + 3\sum_i \phi_i H_i(\omega)}{1 - 2\sum_i \phi_i H_i(\omega)} \tag{9}$$

where

$$H_i(\omega) = \frac{(4\Gamma^\circ/R_i)(2G^*_m + 5G^*_d) + (G^*_d - G^*_m)(16G^*_m + 19G^*_d)}{(40\Gamma^\circ/R_i)(G^*_m + G^*_d) + (2G^*_d + 3G^*_m)(16G^*_m + 19G^*_d)} \tag{10}$$

When (Γ°/R) is set to zero in eq 10, the resulting expression will be denoted by H_0 and the corresponding prediction from eq 9 will be termed G^*_0. The contribution of the interface to the dynamic modulus can then be defined following Lacroix et al.[21] as follows.

$$G^*_{int}(\omega) = G^*(\omega) - G^*_0(\omega) \tag{11}$$

2.1. Determination of the Interfacial Tension from Blend Rheology. Several groups[16−21] have used these models to study the rheology of polymer blends and determine the equilibrium interfacial tension. The models of Oldroyd and of Choi and Schowalter describe only the low-frequency region of the dynamic storage modulus curve. Graebling and co-workers[20] showed that

Table 1. Properties of Constituents at 230 °C

material	M_n	η_0 (Pa s)	relaxation time (s)
B3	18 000	860	0.002
PP	54 000	1150	0.35
3001	76 000	3000	1.1
3002	63 000	1970	1.3
3150	42 000	490	0.28

Palierne's model[12] may be used to describe the dynamic moduli over a broader frequency range. If each of the blend components is described by a single relaxation time Maxwell model, and if a monodisperse particle size distribution is assumed, eq 9 leads to a distinct plateau at the lower frequencies as depicted by Graebling and co-workers[20] in Figure 1 of their paper.

The location and magnitude of the secondary plateau determine the accuracy with which interfacial tension can be estimated from such data. Several parameters determine whether this transition is noticeably flat and whether it occurs well within the accessible frequency range. As the viscosity ratio k is increased, the secondary plateau moves toward lower storage moduli and lower frequency. As the interfacial tension is reduced, the secondary plateau shifts toward lower frequencies and its width increases. The mean particle size has the opposite effect; broader particle size distributions lead to a less distinct transition. As the ratio of component relaxation times χ approaches 1, the secondary plateau becomes ill-defined. As the volume fraction of the disperse phase is increased, the secondary plateau becomes more pronounced in width and shifts toward higher frequencies. In some cases, where the plateau is ill defined, it is possible to enhance the resolution by evaluating the contribution of the interface to the dynamic storage modulus from both predicted and experimental values of the blend storage modulus,[19,21] as in eq 11. This is described in more detail in the discussion of results of this paper.

3. Experimental Section

3.1. Materials. Nylon-6 (Ultramid B3 from BASF Corporation), neat polypropylene (Profax 6501 from Montell Corporation), and three different grades of maleated polypropylene (PB3001, PB3002, and PB3150, from Uniroyal Chemicals) were used in the study. The three grades of maleated polypropylene contained different amounts of maleic anhydride functionality on polypropylenes with different molecular weights. The maleic anhydride content of PB3001, PB3002, and PB3150 was reported to be 0.15, 0.3, and 0.8 wt %, respectively. This information may be combined with the molecular weights presented in Table 1 to arrive at estimates of 1, 2, and 3 maleic groups per chain in the different polypropylene grades.

3.2. Blending. Blends were prepared with nylon-6 as the matrix and different polypropylenes as the dispersed phase. The materials were dried under a nitrogen blanket for 6−8 h at a temperature of 120 °C, to minimize the effects of moisture. Blends containing 10 and 20 wt % of the disperse phase were prepared in a ZSK-30 twin screw extruder at a temperature of 230 °C for all the zones. The extrudate strands were pelletized and dried.

3.3. Rheological Characterization. Rheological characterization of the blends was carried out at 230 °C on an RMS-800 rheometer with a 50 mm parallel plate arrangement. The disks were prepared by compression molding the pellets in a Carver press under a force of 6 tons and 230 °C. The pellets were predried in a vacuum oven for 10−12 h. The instrument oven was purged with dry nitrogen during measurements to avoid degradation. A frequency range of 0.05−50 rad/s and strains of 10−15% were applied during the measurements. A strain sweep was carried out to determine the limit on the strain for linear viscoelastic response. The phase angle was checked at lower frequencies to avoid data where the phase angle is too close to 90°, making it inaccurate.

3.4. Morphology Analysis. The samples for examination of blend morphology were prepared by placing the prenotched disks in the RMS 800 oven, heating them to 230 °C, and placing them directly in liquid nitrogen. Those were then fractured under liquid nitrogen. The fractured specimens were then etched in dichlorobenzene at 120 °C to dissolve the polypropylene phase. The etched samples were then examined in a Phillips Electroscan 2020 environmental scanning microscope. A minimum of 400 particles and nearly 1000 particles in some cases were examined in each micrograph to obtain particle size distributions and the volume average radii for each case.

4. Results and Discussion

4.1. Blend Morphology. The micrographs of two nonreactive blends (90/10 and 80/20) are presented in Figure 1a,b while the micrographs of three pairs of reactive blends are presented in Figure 1c−h. The reactive blend specimens were all etched, but the two nonreactive blend specimens were not. The particles are roughly spherical in all cases. Particle radii in the nonreactive blends are of the order of 10 μm while particle radii in the reactive blends are of the order of 1 μm. Particle size distributions obtained with different extents of polymer reaction are compared for 90/10 blends in Figure 2 and for 80/20 blends in Figure 3. These distributions are based on volume fraction. Figure 2 shows that, among the 90/10 blends, the one with the higher maleated site density on PP has a much narrower distribution as well as a smaller volume average particle size. However, among the 80/20 blends, as shown in Figure 3, the breadth of the distribution is very similar, and the volume average particle sizes are close, too. The latter pair of 80/20 blends is particularly interesting in the following discussion of blend rheology.

4.2. Blend Rheology. The storage modulus curves of the different constituents are presented in Figure 4, and the corresponding loss modulus curves are presented in Figure 5. The zero-shear viscosity η_0 and a characteristic relaxation time have been determined from these data and are listed in Table 1 for each of the components. It should be noted that the relaxation time of the matrix is significantly lower than that of the disperse phase. This is important to identify changes in relaxation times brought about by the changes occurring at the interface with different values of reactive site density.

To observe the broad rheological changes brought about by the interfacial reaction, we examine the effect of increased extent of maleation (causing greater extents of reaction) for the same weight fraction of the disperse phase. It must be noted that the amount of amine functionality available in the matrix for interfacial reaction is much more than the amount of maleic anhydride in the polypropylene. Hence, any maleic anhydride at the interface is completely reacted. Furthermore, among the 80/20 reactive blends, the particle size distributions are similar (see Figure 3), so that the effect of varying extent of interfacial reaction on the blend rheology may be investigated at constant particle size. This is not the case for the 90/10 reactive blends.

4.3. Determination of the Interfacial Tension. The interfacial tension is determined by combining the particle size distribution with the storage modulus curves in eqs 9 and 10. We confirmed the validity of our

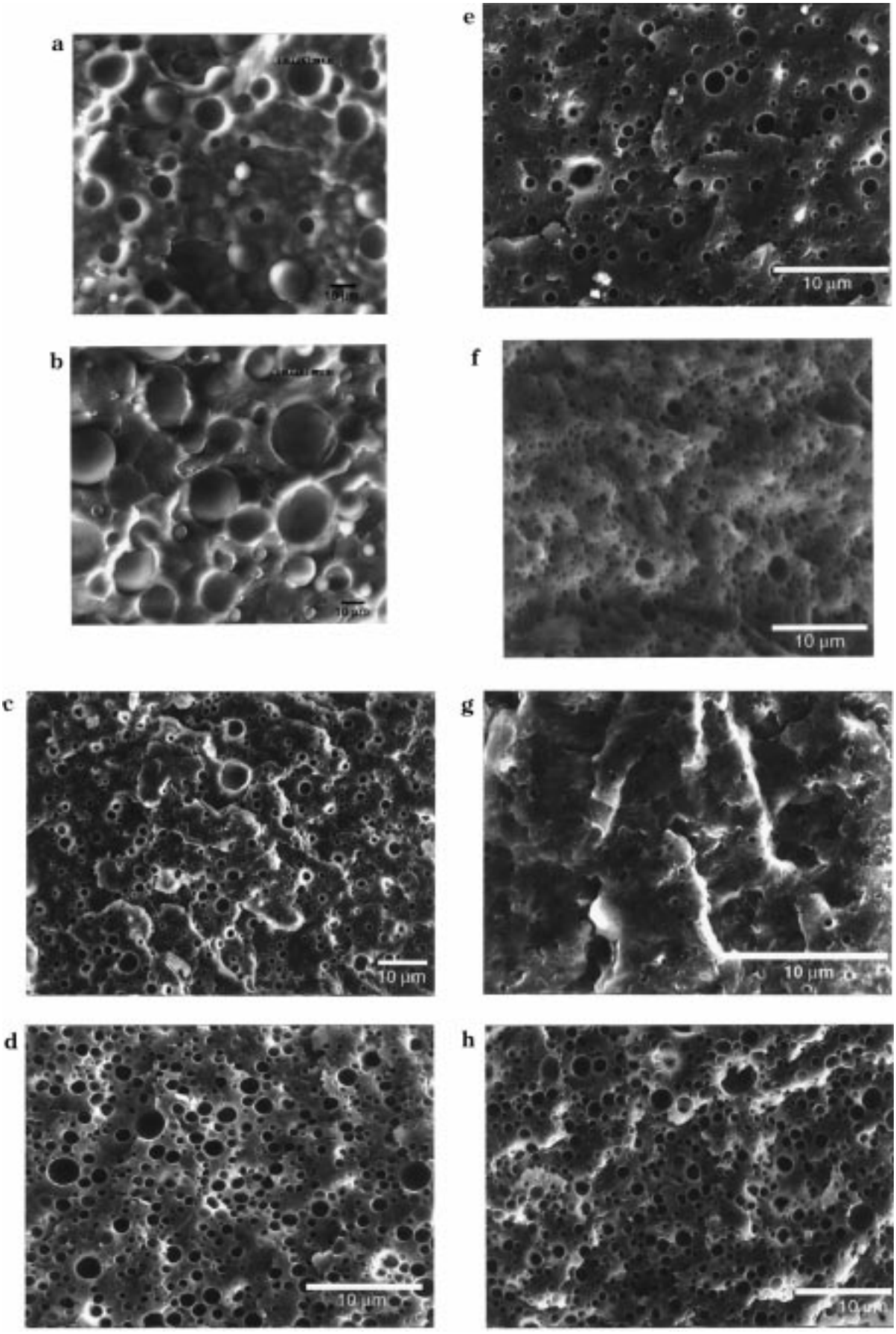

Figure 1. Morphology of blends with nylon-6 (B3) as matrix and a neat PP as well as three different grades of maleated polypropylene: (a) B3/PP 90/10 by weight, (b) B3/PP 80/20, (c) B3/3001 90/10, (d) B3/3001 80/20, (e) B3/3002 90/10, (f) B3/3002 80/20, (g) B3/3150 90/10, and (h) B3/3150 80/20.

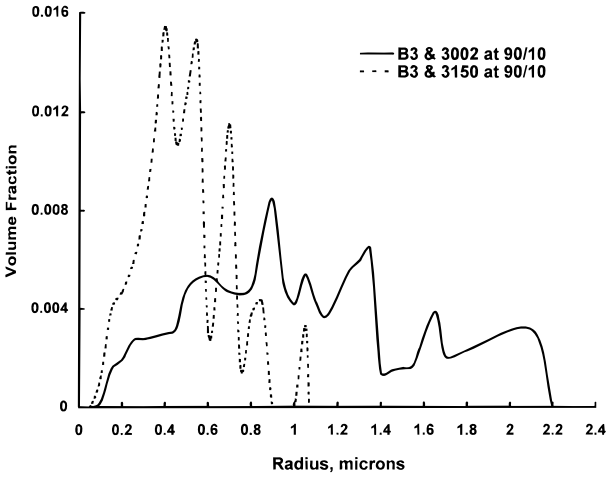

Figure 2. Comparison of particle size distributions by volume for two 90/10 blends: B3/3002 and B3/3150.

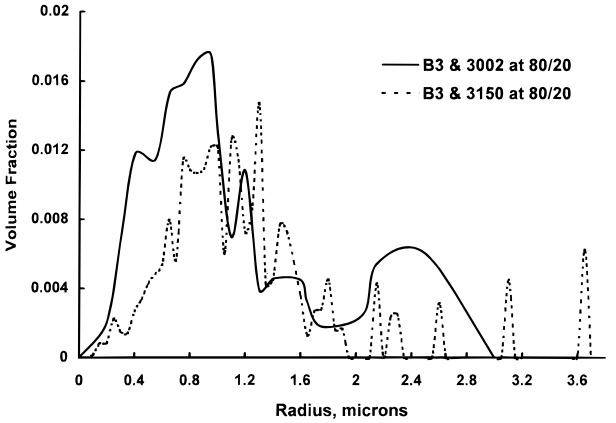

Figure 3. Comparison of particle size distributions by volume for two 80/20 blends: B3/3002 and B3/3150. Note the similar breadth of the two distributions.

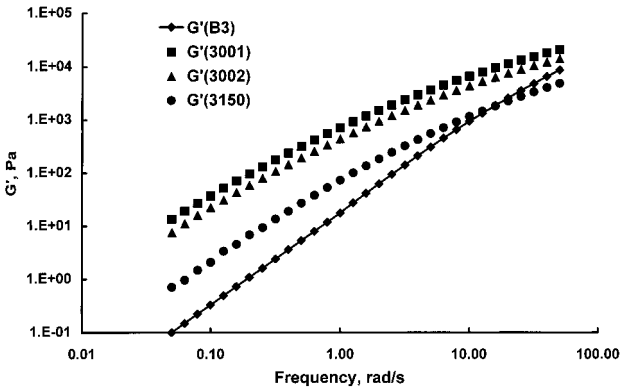

Figure 4. Comparison of the dynamic storage modulus curves of different blend components in shear.

procedure for estimating the equilibrium interfacial tension, with rheological measurements on polypropylene−polystyrene blends in our laboratory. A value of 5 mN/m was obtained for this system, which agrees well with the values reported in the literature.[21] The same procedure yielded an estimate of 10 mN/m for the nonreactive blends of nylon-6 with polypropylene.

Figure 6 shows a comparison of the model predictions with the experimentally obtained storage modulus curves and loss modulus curves for the 90/10 blend of B3 and 3001. This is the least reactive system as it is the least maleated. A value of 10 mN/m for Γ° gives a

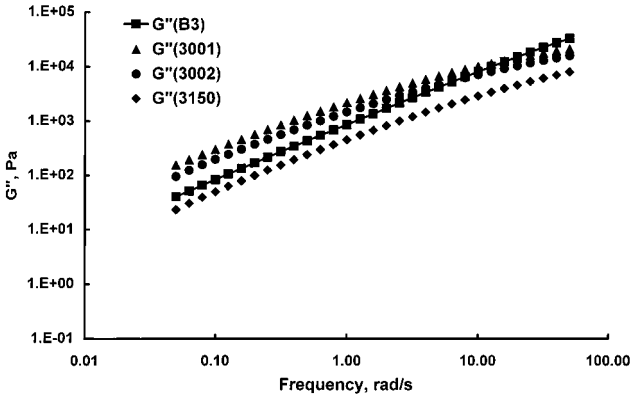

Figure 5. Comparison of the dynamic loss modulus curves of the different blend components in shear.

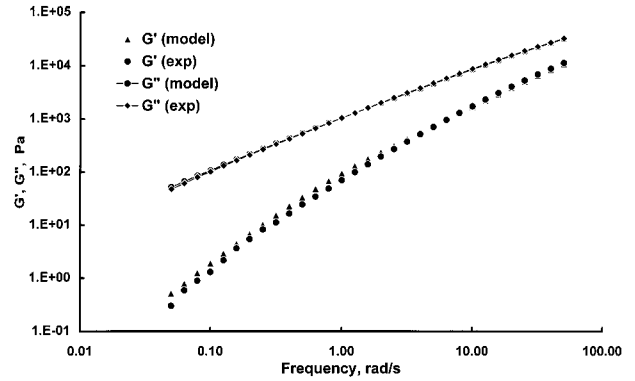

Figure 6. Fit of the dynamic storage modulus data to Palierne's theory for the 90/10 blend of B3 and 3001 with Γ° = 10 mN/m; $\bar{R}_v = 2.53$ μm.

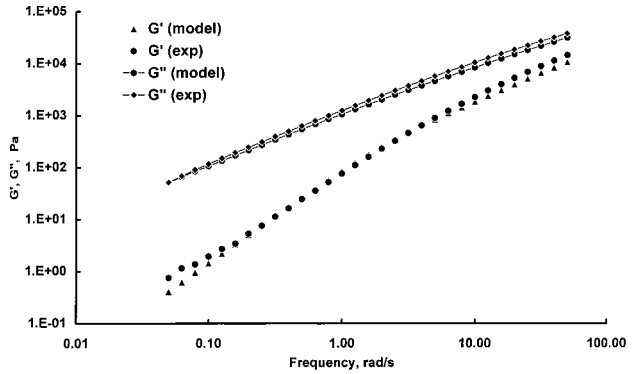

Figure 7. Fit of the dynamic storage modulus data to Palierne's theory for the 90/10 blend of B3 and 3002 with Γ° = 8 mN/m; $\bar{R}_v = 1.14$ μm.

good fit between the model and the experimentally obtained values. Figure 7 shows a similar fit for the storage and the loss moduli of the B3/3002 (90/10) system with a value of 8 mN/m for Γ°. The first fit for the 90/10 blend of B3 and 3150 presented in Figure 8 is labeled $\beta = 0$, a parameter associated with the interfacial shear modulus and defined in the following paragraph. The fit is good at moderate to high frequencies with Γ° = 3 mN/m, but the fit is inadequate at low frequencies. This may be seen more clearly on a plot of the contribution of the interface to the dynamic storage modulus as defined in eq 11. The interface contribution G'_{int} is evaluated with eq 11 for both experimental data and the model predictions, and the two are compared in Figure 9. Use of several particle size fractions to represent the particle size distribution did not improve

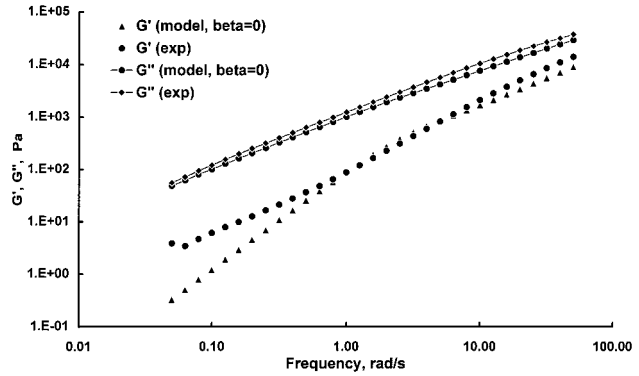

Figure 8. Fit of the dynamic storage modulus data to Palierne's theory for the 90/10 blend of B3 and 3150 with $\Gamma° = 3$ mN/m and $\beta = 0$; $\bar{R}_v = 0.55$ μm.

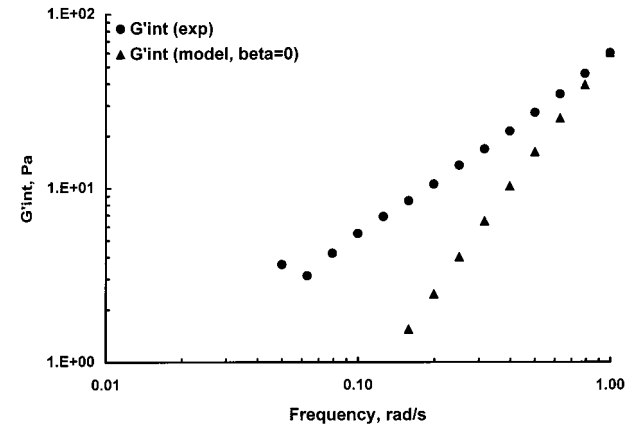

Figure 9. Comparison of interface contribution to dynamic storage modulus at lower frequencies from experiments and from Palierne's theory for the 90/10 blend of B3 and 3150 with $\Gamma° = 3$ mN/m and $\beta = 0$.

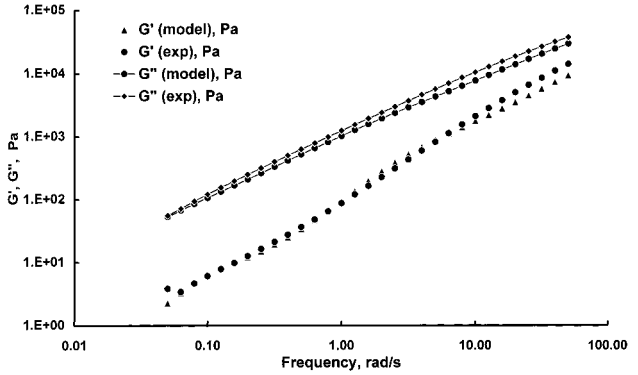

Figure 10. Fit of the dynamic storage modulus data to Palierne's theory for the 90/10 blend of B3 and 3150 with $\Gamma° = 3$ mN/m and $\beta_0 = 0.1$ mN/m; $\bar{R}_v = 0.55$ μm.

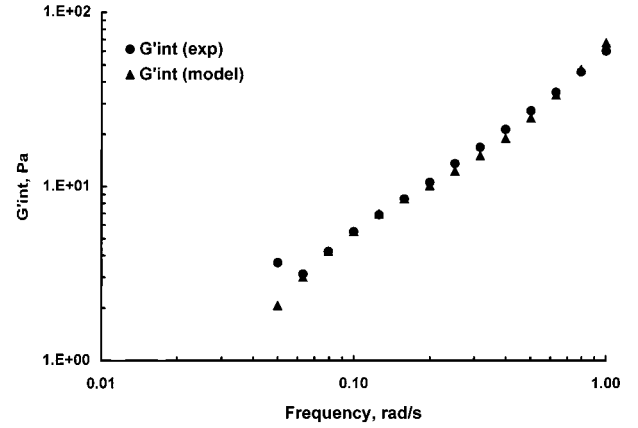

Figure 11. Comparison of interface contribution to dynamic storage modulus at lower frequencies from experiments and from Palierne's theory for the 90/10 blend of B3 and 3150 with $\Gamma° = 3$ mN/m and $\beta_0 = 0.1$ mN/m.

the low-frequency fit. It should be stated at this stage that the storage modulus in the lower frequency range is the main focus of discussion as this is most susceptible to the changes in the interface.

We now turn to other mechanical characteristics of the interface besides the equilibrium interfacial tension. The surface dilatation modulus $\beta^*_d(\omega)$ is usually associated with nonuniformity of the interface, and the surface shear modulus $\beta^*_s(\omega)$ is associated with the resistance to the shear deformation. It will be assumed that, in the melt blends of this study, the interface is uniformly occupied by the reaction products so that the surface dilatation modulus can be ignored. However, the reaction product does resist shear deformation, and its surface shear modulus $\beta^*_s(\omega)$ should be accounted for. The shear modulus $\beta^*_s(\omega)$ of the interfacial reaction product consists of the storage and loss moduli, $\beta'_s(\omega)$ and $\beta''_s(\omega)$, respectively. In the present work, estimates of these quantities are obtained from the theory of lightly cross-linked rubber.[22] In the framework of this two-parameter theory,

for $\omega\lambda_\beta < 1$:

$$\beta'_s = \beta_0$$
$$\beta''_s = \beta_0\omega\lambda_\beta \quad (12)$$

for $\omega\lambda_\beta > 1$:

$$\beta'_s = \beta''_s = \beta_0\sqrt{\omega\lambda_\beta} \quad (13)$$

The quantity β_0 is a low-frequency plateau in the storage modulus for the reaction product, and λ_β is a characteristic relaxation time. The transition frequency $1/\lambda_\beta$ may be identified on a plot of the interface contribution G'_{int} to the experimental storage modulus for the blend, as the frequency at which this contribution changes slope. Incorporating the quantity $\beta^*_s(\omega)$ in eq 9 leads to a dramatic improvement in the agreement between the experimental and model curve in reactive blends. This is shown in Figures 10 and 11 for the B3/3150 (90/10) blend with $\beta_0 = 0.1$ mN/m and λ_β around 1 s.

Fits of rheological data for the 80/20 blends are all done with both the interfacial tension and the new parameters for interfacial shear modulus. The values of interfacial tension are the same as the values found from the corresponding 90/10 blends. These fits are presented in Figures 12 and 13 for the B3/3001 (80/20) blend, in Figures 14 and 15 for the B3/3002 (80/20) blend, and in Figures 16 and 17 for the B3/3150 (80/20) blend. The fits for the latter two blends are particularly interesting because as seen in Figure 3, their particle size distributions are very similar. The values $\beta_0 = 0.1$ mN/m and $\lambda_\beta = 0.8$ s are used for both blends, but the interfacial tension value is reduced from 8 mN/m for the B3/3002 to 3 mN/n for the B3/3150 blend. This yields a very good fit for the interface contribution to the storage modulus of both systems at lower frequencies.

4.4. Reactive Sites. The reactive site concentrations in different constituents have been calculated with the

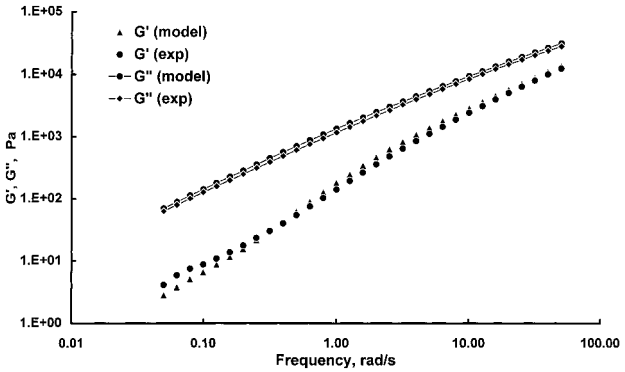

Figure 12. Fit of the dynamic storage modulus data to Palierne's theory for the 80/20 blend of B3 and 3001 with $\Gamma^\circ = 10$ mN/m and $\beta_0 = 0.4$ mN/m; $\bar{R}_v = 1.44$ μm.

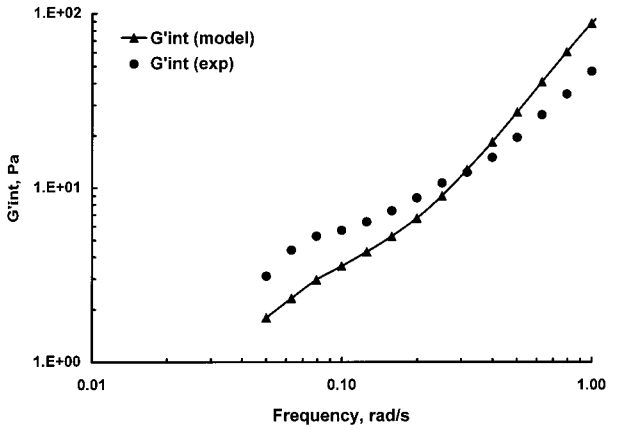

Figure 13. Comparison of interface contribution to dynamic storage modulus at lower frequencies from experiments and from Palierne's theory for the 80/20 blend of B3 and 3001 with $\Gamma^\circ = 10$ mN/m and $\beta_0 = 0.4$ mN/m.

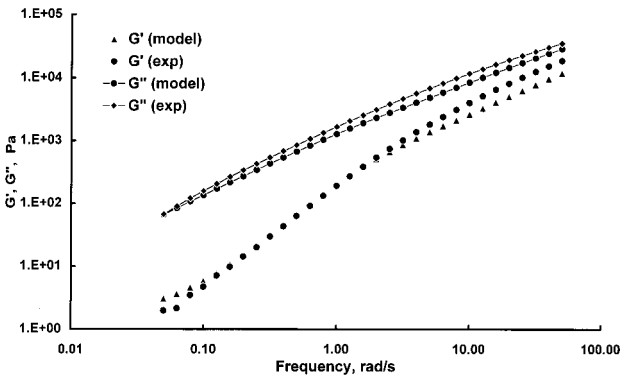

Figure 14. Fit of the dynamic storage modulus data to Palierne's theory for the 80/20 blend of B3 and 3002 with $\Gamma^\circ = 8$ mN/m and $\beta_0 = 0.1$ mN/m; $\bar{R}_v = 1.44$ μm.

help of data from Table 1, and the results are tabulated in Table 2. As seen in Table 2, the amount of amine functionality available for interfacial reaction is much more than the amount of maleic anhydride. This is important as it ensures that the interfacial reaction goes to completion and is not limited by the amount of amine available. That is, any maleic anhydride at the interface is completely reacted. The number of maleic anhydride groups per chain available for reaction increases from 1 per chain in PB3001 to 3.4 in PB3150. This is a significant difference that explains the greater enhancement in storage modulus and relaxation times for reactive blends with progressively increasing extent of reaction. Combining the information in Table 2 with

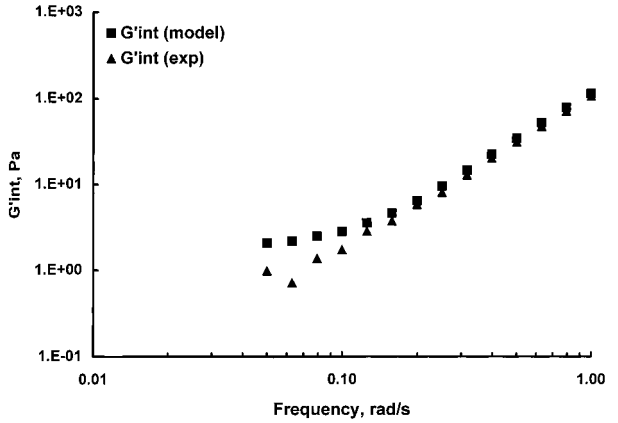

Figure 15. Comparison of interface contribution to dynamic storage modulus at lower frequencies from experiments and from Palierne's theory for the 80/20 blend of B3 and 3002 with $\Gamma^\circ = 8$ mN/m and $\beta_0 = 0.1$ mN/m.

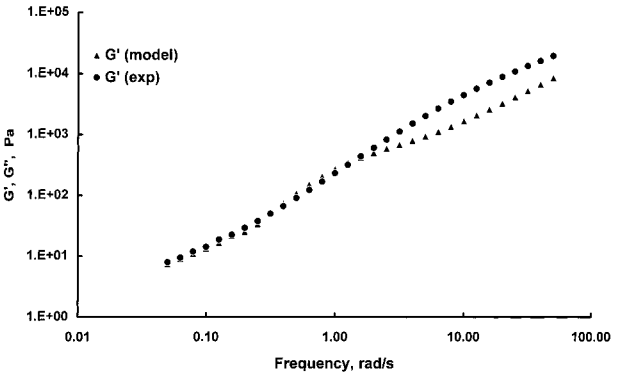

Figure 16. Fit of the dynamic storage modulus data to Palierne's theory for the 80/20 blend of B3 and 3150 with $\Gamma^\circ = 3$ mN/m and $\beta_0 = 0.1$ mN/m; $\bar{R}_v = 1.56$ μm.

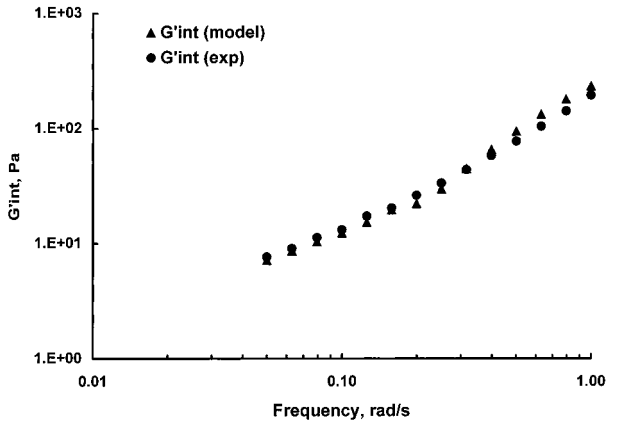

Figure 17. Comparison of interface contribution to dynamic storage modulus at lower frequencies from experiments and from Palierne's theory for the 80/20 blend of B3 and 3150 with $\Gamma^\circ = 3$ mN/m and $\beta_0 = 0.1$ mN/m.

estimates of the equilibrium interfacial tension, it is seen that the interfacial tension drops continuously with increasing reaction and increasing occupation of the interface. This would indicate that maximum coverage is not reached in the reactive blends with components selected for this study. The different grades of maleated polypropylene used in this study had different molecular weight distributions in addition to different extents of maleation. More direct evaluation of the effect of interfacial reaction alone might be obtained with more uniform molecular weight distributions of the polypro-

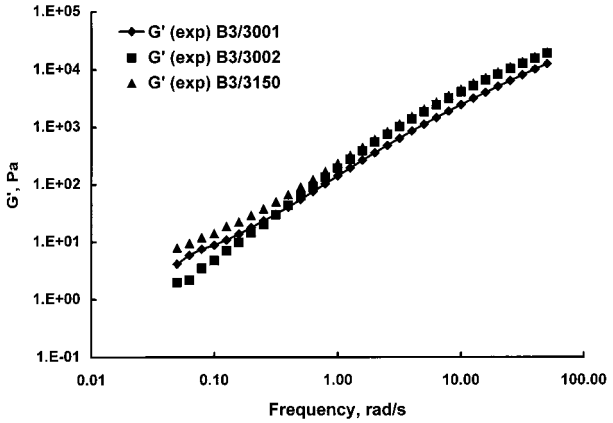

Figure 18. Comparison of the dynamic storage modulus curves for 80/20 blends of B3 with the three different maleated polypropylenes.

Table 2. Reactive Site Concentration in Different Materials

material		*n* (no. of MAH/chain)
B3	15.74 (g-mol of amines/kg of B3)	
3001	0.015 (g-mol of MAH/kg of 3001)	1
3002	0.030 (g-mol of MAH/kg of 3002)	2
3150	0.080 (g-mol of MAH/kg of 3150)	3.4

pylene specimens with different extents of maleation.

5. Conclusions

The results of this study show that a polymer reaction at the interface in reactively compatibilized polymer blends leads to a reduction in particle size of the dispersed phase as well as a reduction in interfacial tension. The number of reactive sites for grafts per maleated polypropylene chain goes from 1 to 2 to 3.4 in these systems. The extent of polymer reaction at the interface affects the phase morphology differently at different phase volume fractions. The equilibrium interfacial tension drops progressively from 10 mN/m in nonreactive blends to 8 mN/m and then to 3 mN/m in reactive blends with increasing extent of reaction. Among the 90/10 blends, the one with the higher maleated site density on PP has a much narrower distribution as well as a smaller volume average particle size, indicating that the degree of stabilization increases with the level of reaction product in these blends. However, among the 80/20 blends, as shown in Figure 3, the breadth of the distribution is very similar, and the volume average particle sizes are close, too. Rheological observations show that besides a reduction in interfacial tension, there is an additional relaxation mechanism leading to enhancement in the storage modulus of the reactive blends as compared to the case of the nonreactive blends. This is attributed to the product of the interfacial reaction.

Acknowledgment. This research was supported in part by the State of Michigan through a REF grant administered by the Composite Materials and Structures Center at Michigan State University and through a grant from Montell Polyolefins and the Michigan Materials and Processing Institute. The authors are pleased to acknowledge the contribution by Dr. Richard Schalek at Michigan State University, in scanning electron microscopy, and the donation of materials for this study by Montell Polyolefins, Uniroyal Chemicals, and BASF.

References and Notes

(1) Paul, D. R.; Barlow, J. W.; Keskkula, H. In *Encyclopedia of Polymer Science and Engineering*, 2nd ed.; Kroschwitz, J. I., Ed.; Wiley: New York, 1988; Vol. 12.
(2) Cho, K.; Jeon, H. K.; Park, C. E.; Jim, J.; Kim, K. U. *Polymer* **1996**, *37* (7), 1117.
(3) Elemans, P. H. M.; Janssen, J. M. H.; Meijer, H. E. H. *J. Rheol.* **1991**, *34* (8), 1311.
(4) Brahimi, B.; Ait-Khadi, A.; Ajji, A.; Jerome, R.; Fayt, R. *J. Rheol.* **1991**, *35* (6).
(5) Wu, S. *Polym. Eng. Sci.* **1987**, *27*, 335.
(6) Helfand, E.; Tagami, Y. *Polym. Lett.* **1971**, *9*, 741−746.
(7) Fayt, R.; Jerome, R.; Teyssie, Ph. *J. Polym. Sci., Polym. Lett. Ed.* **1986**, *24*, 25.
(8) O'Shaughnessy, B.; Sawhney, U. *Macromolecules* **1996**, *29*, 7230.
(9) Sundararaj, U.; Macosko, C. W. *Macromolecules* **1995**, *28*, 2647.
(10) Frankel, N. A.; Acrivos, A. *Chem. Eng. Sci.* **1967**, *22*, 847−853.
(11) Schowalter, W. R.; Chaffey, C. E.; Brenner, H. *J. Colloid. Interface Sci.* **1968**, *26*, 152.
(12) Palierne, J. F. *Rheol. Acta* **1990**, *29*, 204−214.
(13) Loewenberg, M.; Hinch, E. J. *J. Fluid Mech.* **1996**, *321*, 395−419.
(14) Oldroyd, J. G. *Proc. R. Soc. London, A* **1953**, *218*, 122−132.
(15) Choi, S. J.; Schowalter, W. R. *Phys. Fluids* **1975**, *18*, 420−427.
(16) Scholz, P.; Froelich, D.; Muller, R. *J. Rheol.* **1989**, *33* (3), 481−499.
(17) Graebling, D.; Muller, R. *J. Rheol.* **1990**, *34* (2).
(18) Graebling, D.; Muller, R. *Colloids Surf.* **1991**, 89−103.
(19) Gramespacher, H.; Meissner, R. *J. Rheol.* **1992**, *36* (6), 1127.
(20) Graebling, D.; Muller, R.; Palierne, J. F. *Macromolecules* **1993**, *26*, 320−329.
(21) Lacroix, C.; Aressy, M.; Carreau, P. J. *Rheol. Acta* **1997**, *36*, 416.
(22) Ferry, J. D. *Viscoelastic Properties of Polymers*, 3rd ed.; John Wiley and Sons: New York, 1980.
(23) Edwards, D. A.; Brenner, H.; Wasan, D. T. *Interfacial Transport Processes and Rheology*; Butterworth-Heinemann: Woburn, MA, 1991.

MA980181D